Mater. Res. Soc. Symp. Proc. Vol. 1198 © 2010 Materials Research Society 1198-E07-22

Magnetic and Electronic Properties of $Fe_{0.1}Sc_{0.9}N$ /ScN(001)/MgO(001) Grown by Radio-Frequency Molecular Beam Epitaxy

Costel Constantin,[1] Kangkang Wang,[2] Abhijit Chinchore,[2] Han-Jong Chia[3], John Markert[3], Arthur R. Smith,[2]

[1]Department of Physics, Seton Hall University, South Orange, NJ 07079

[2]Nanoscale & Quantum Phenomena Institute, Department of Physics and Astronomy, Ohio University, Athens, OH 45701

[3]Department of Physics, University of Texas at Austin, Austin, TX 78712

ABSTRACT

$Fe_{0.1}Sc_{0.9}N$ with a thickness of ~ 380 nm was grown on top of a ScN(001) buffer layer of ~ 50 nm, grown on MgO(001) substrate by radio-frequency N-plasma molecular beam epitaxy (rf-MBE). The buffer layer was grown at T_S ~ 800 ^oC, whereas the $Fe_{0.1}Sc_{0.9}N$(001) film was grown at T_S ~ 420 °C. In-situ reflection high-energy electron diffraction measurements show that the $Fe_{0.1}Sc_{0.9}N$ film growth starts with a combination of spotty and streaky pattern [indicative of a combination of smooth and rough surface]. After ~ 10 minutes of growth, the pattern converts to a spotty one [indicative of a rough surface]. Towards the end of the $Fe_{0.1}Sc_{0.9}N$ film growth, the spotty pattern transforms into even spottier, but also ring-like indicating a polycrystalline behavior. Superconducting quantum interference device magnetic measurements show a ferromagnetic to paramagnetic transition of T_C ~ 370 – 380 K. We calculated a magnetic moment per atom of $\mu^{(Fe_{0.1}Sc_{0.9}N)} = 0.037$ Bohr magneton/ Fe-atom. Based on the carrier concentration measurements ($n_S^{(Fe_{0.1}Sc_{0.9}N)} = 2.086 \times 10^{19}$ /cm^3), we find that iron behaves as an acceptor. Comparisons are made with similar MnScN (001)/ScN(001)/MgO(001) system.

INTRODUCTION

Recently, many efforts have been focused to obtaining III-V dilute magnetic semiconductors (DMS) by doping semiconductors, such as gallium nitride (GaN) and gallium arsenide (GaAs), with transition metal manganese (Mn) [1-12]. To use DMS materials in spintronics applications, the materials should exhibit a ferromagnetic transition temperature (T_C) above 300 K. However, up to date, the experimental results reported the growth and magnetic properties of MnGaN with no convincing confirmation of T_C at or above 300 K [1-8]. Haider et al. [7] in particular, indicate clearly that N-rich and slight metal-rich growth regimes of MnGaN result in ferromagnetism above 300 K. Nevertheless, the origin of ferromagnetism in this result is not fully understood. The T_C reported values for MnGaAs could not be raised beyond 110 K [9], which remained a standard for this material for many years. Post-growth annealing treatments proved to be the way to surpass this barrier [10]. Nevertheless, the highest reported values of T_C in MnGaAs remain only around 173 K [10, 11]. It is obvious that there are still challenges in obtaining a reliable above-room-temperature DMS. Therefore, the quest for finding new possible DMSs is in full swing. One interesting new system is iron doped scandium nitride (FeScN). Scandium nitride (ScN) is a semiconductor with a rocksalt crystal structure, a

direct band gap of 2.15 eV, and an indirect band gap of 0.9 - 1.1 eV [13-18]. In the past it had been shown that manganese alloys very well with ScN, namely Al-Brithen *et al*. showed that manganese scandium nitride (MnScN) alloy follows the Vegard's law, with the two tetragonal lattice constants of the Mn-rich end linearly approaching the single cubic lattice constant at the Sc-rich end [19]. Moreover, recent theoretical calculations predict a T_C for MnScN alloys above 350 K, when ScN is doped with up to 20% Mn [20-22]. Our group experimentally found that 3% and 5% Mn-doped ScN showed ferromagnetism past 350 K [23].

In this article, we focus in particular on the magnetic and electronic properties of $Fe_{0.1}Sc_{0.9}N(001)$ grown on a buffer of ScN(001) grown on MgO(001) substrate by radio-frequency molecular beam epitaxy (rf-MBE). During the growth, the reflection high-energy electron diffraction (RHEED) measurements reveal a surface transformation that starts with a combination of smooth and rough growth (for the first ~ 10 minutes of growth). As the growth progresses towards the end, the surface becomes even rougher, and with a polycrystalline behavior. Magnetic measurements show a ferromagnetic to paramagnetic transition of T_C ~ 370 – 380 K, and with a magnetic moment per atom of $\mu^{(Fe_{0.1}Sc_{0.9}N)} = 0.037\ \mu_B$/Fe-atom. Carrier concentration was measured to be $n_S^{(Fe_{0.1}Sc_{0.9}N)} = 2.086 \times 10^{19}$ /cm^3, and with a corresponding mobility value of $\mu_S^{(Fe_{0.1}Sc_{0.9}N)} = 73.44$ cm^2/(Vs).

EXPERIMENT

The rf-MBE chamber uses N_2 as a source gas, and employs effusion cells for Sc and e-beam cell for Fe evaporation. During the entire growth, the N plasma source is kept constantly operating at 500 W and with a N_2 flow rate set at 1.1 sccm ($P_{chamber} = 9 \times 10^{-6}$ Torr). The substrate temperature is measured *in-situ* by using a thermocouple, which is located behind the substrate heater and *ex-situ* by using an infrared pyrometer which is looking through a glass window directly at the front side of the sample. The $Fe_{0.1}Sc_{0.9}N$ layer is grown at a specific cation flux ratio $r = J_{Fe} / (J_{Sc} + J_{Fe})$, with $J_{Fe} = 1.67 \times 10^{13}$ cm^{-2}s^{-1}, and J_{Sc} ~ 1.5×10^{14} cm^{-2}s^{-1}. The film is monitored *in-situ* by a Staib RHEED instrument with an e-beam energy of 20 keV. After the sample is exposed to ambient it is measured with a Quantum Design superconducting quantum interference device (SQUID), and a homemade four-point probe (Van der Pauw geometry) resistivity/Hall effect measurements system (R-T/Hall effect).

RESULTS AND DISCUSSIONS

Shown in Fig. 1 (a – h) are the RHEED patterns of the $Fe_{0.1}Sc_{0.9}N(001)$/ScN(001)/MgO(001) film taken at [110] & [100] crystal orientation of the MgO(001) substrate. After the MgO(001) substrate was ultrasonically cleaned with acetone and isopropanol, it had been loaded into the MBE chamber and deoxidized by heating and nitridation at a temperature of ~ 900 °C for 30 minutes, while keeping the N_2 flow rate to 1.1 sccm and rf-plasma power at 500 W. Immediately after this, the RHEED patterns shown in Figs. 1 (a) & (b) look streaky, indicating a suitably smooth substrate surface.

Next, a buffer layer of ScN is grown at a sample temperature of 800 °C and with thickness t_{ScN} ~ 50 nm. The RHEED patterns of the ScN buffer layer [Figs. 1 (c) & (d)] indicate a relatively smooth starting substrate, despite being very thin. At the end of the buffer layer growth, the substrate temperature is lowered to T_S ~ 420 °C, and the growth of the $Fe_{0.1}Sc_{0.9}N$ film starts by simultaneously opening the Fe and Sc shutters while keeping the plasma source

opened at 1.1 sccm and 500 W power. The growth run that we performed for the $Fe_{0.1}Sc_{0.9}N$ film starts with a combination of spotty and streaky RHEED patterns [Figs. 1 (e) & (f)]; we generally find that the pattern converts to a spotty one after some time (~ 10 minutes). At the end of the $Fe_{0.1}Sc_{0.9}N$ film growth the RHEED patterns [Figs. 1 (g) & (h)] transform into even spottier, but also ring-like indicating a polycrystalline behavior.

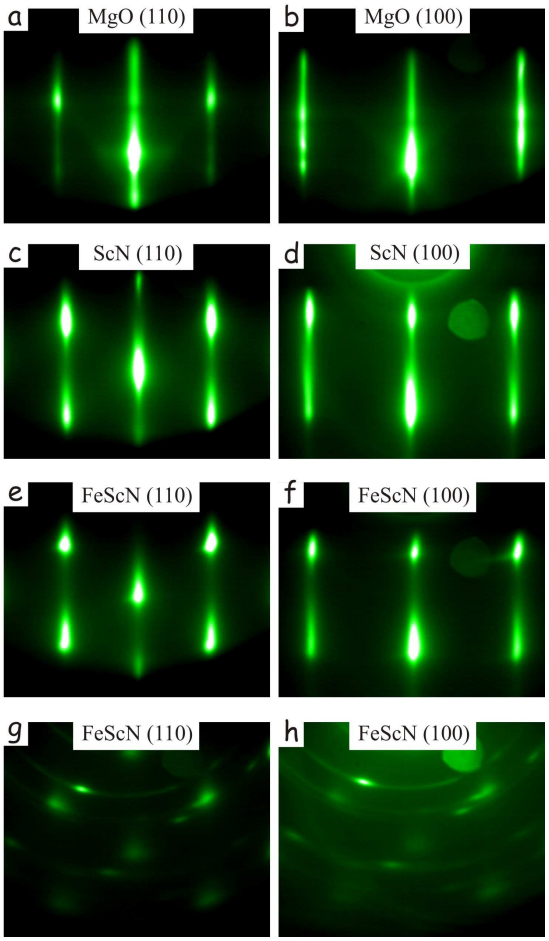

Figure 1. (a) & (b) RHEED patterns of MgO(001) substrate taken before the ScN buffer layer growth. (c) & (d) RHEED patterns of ScN(001) buffer layer taken before the FeScN film growth. (e) & (f) RHEED patterns of $Fe_{0.1}Sc_{0.9}N$ taken ~ 5 minutes after Sc and Fe shutters have been opened. (g) & (h) RHEED patterns taken at the end of a ~ 380 nm growth of $Fe_{0.1}Sc_{0.9}N$ film. The left column of RHEED patterns [i.e., (a), (c), (e), and (g)] were taken along the [110] MgO substrate crystal orientation, whereas the right column of RHEED patterns were taken along [100] MgO substrate crystal orientation [i.e., (b), (d), (f), and (h)].

In Fig. 2 we present the magnetic behavior of the $Fe_{0.1}Sc_{0.9}N(001)$ which was measured by SQUID. The initial raw magnetic data for both Fig. 2 (a) and (b) has been corrected by performing a background subtraction of the paramagnetic signal originating from the sample holder and the MgO substrate. The magnetic signal presented in Fig. 2 (a) starts saturating at a field of ~ 4000 Oe and it maintains a saturation average value of ~ 1.51 emu/cm^3 up to maximum field of 20000 Oe.

In Fig. 2 (a) we also observe a remanence of ~ 0.060 emu/cm^3 and a coercive field of ~ 50 Oe. These results differ from the magnetic results we obtained for a work-in-progress Mn-doped ScN system that we grew in our lab [23]. We observed that for MnScN films $Mn_{0.03}Sc_{0.97}N$, and $Mn_{0.05}Sc_{0.95}N$ the hysteresis was saturated at 0.746 emu/cm^3, and 0.309 emu/cm^3, respectively. Magnetic saturation is achieved at ~ 2500 Oe for both MnScN samples. While $Mn_{0.03}Sc_{0.97}N$ does not show any measurable remanent magnetization, the $Mn_{0.05}Sc_{0.95}N$ sample shows about 0.044 emu/cm^3 at remanence and a coercive field of about 425 Oe.

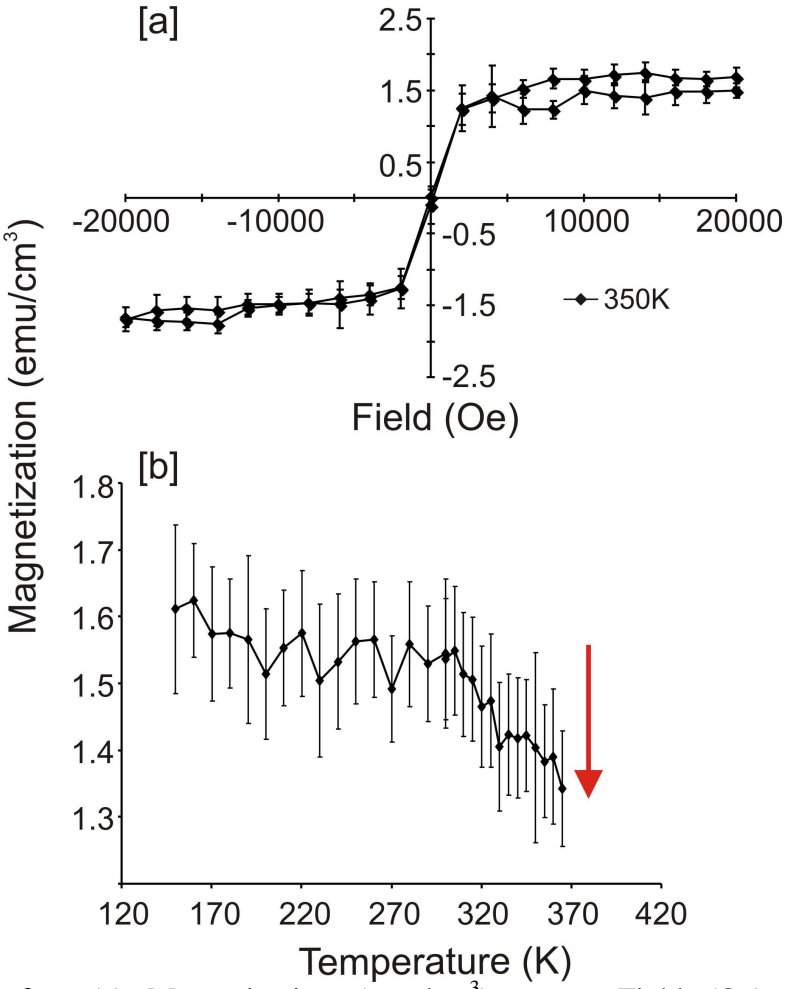

Figure 2. (a) Magnetization (emu/cm^3) versus Field (Oe) for $Fe_{0.1}Sc_{0.9}N$ film. (b) Magnetization (emu/cm^3) versus Temperature (K) for $Fe_{0.1}Sc_{0.9}N$ film. The red arrow in (b) indicates the estimated T_C for $Fe_{0.1}Sc_{0.9}N$ film.

In Fig. 2 (b), we present the magnetization versus temperature done under applied field, and one can clearly see a monotonic decrease of net magnetization starting from ~ 150 K all the way up to above 300 K. The ferromagnetic to paramagnetic transition of T_C ~ 370 – 380 K is represented by the red arrow in Fig. 2 (b). Our calculated magnetic moment per atom is $\mu^{(Fe_{0.1}Sc_{0.9}N)} = 0.037\ \mu_B$/ Fe-atom, where $\mu_B = 9.724 \times 10^{-21}$ emu is the Bohr magneton. For MnScN system we found for $Mn_{0.03}Sc_{0.97}N$, and $Mn_{0.05}Sc_{0.95}N$ magnetic moments of $\mu^{(Mn_{0.03}Sc_{0.97}N)} = 0.0617\ \mu_B$/ Mn-atom, and $\mu^{(Mn_{0.05}Sc_{0.95}N)} = 0.0152\ \mu_B$/ Mn-atom, respectively.

The carrier concentration that we measured with our R-T/Hall effect system was found to be $n_S^{(Fe_{0.1}Sc_{0.9}N)} = 2.086 \times 10^{19}$ /cm^3, with a corresponding mobility value of $\mu_S^{(Fe_{0.1}Sc_{0.9}N)} = 73.44$ cm^2/(Vs). Similarly for MnScN system we found for $Mn_{0.03}Sc_{0.97}N$, and $Mn_{0.05}Sc_{0.95}N$ values of $n_S^{(Mn_{0.03}Sc_{0.97}N)} = 4 \times 10^{19}$ /cm^3, and $n_S^{(Mn_{0.05}Sc_{0.95}N)} = 2.18 \times 10^{19}$ /cm^3, with corresponding mobility values of $\mu_S^{(Mn_{0.03}Sc_{0.97}N)} = 24.8$ cm^2/(Vs) and $\mu_S^{(Mn_{0.05}Sc_{0.95}N)} = 33.8$ cm^2/(Vs), respectively. Based on our carrier concentration measurements, we find that Fe atoms behave as acceptors in ScN. For example, a ScN control sample (no iron) has $n_S^{(ScN)} = 2.76 \times 10^{20}$/cm^3, and as we put 10% Fe into it, the carrier concentration value drops by more than an order of magnitude [i.e., $n_S^{(Fe_{0.1}Sc_{0.9}N)} = 2.086 \times 10^{19}$/cm^3]. It is known that ScN has a very high concentration of free carriers due in part to N vacancies [17].

CONCLUSIONS

$Fe_{0.1}Sc_{0.9}N$ was grown on top of ScN(001) buffer layer, grown on MgO(001) substrate by radio-frequency N-plasma molecular beam epitaxy (rf-MBE). Although the growth of $Fe_{0.1}Sc_{0.9}N$ starts with a suitably smooth (2D) surface (obtained at the end of the ScN buffer layer growth) it gets spottier (more 3D) as the growth evolves in time, to culminate with a rough and polycrystalline surface at the end of the growth. Magnetic measurements reveal a ferromagnetic to paramagnetic transition of $T_C \sim 370 - 380$ K, and a magnetic moment per atom of $\mu^{(Fe_{0.1}Sc_{0.9}N)} = 0.037$ Bohr magneton/ Fe-atom. It is interesting to note that both Fe and Mn have very similar responses in the ScN. They both appear to act as p-type dopants. Despite the encouraging T_C value we presented in this article, further experiments need to be done in order to identify the source of ferromagnetism.

ACKNOWLEDGEMENTS

This collaborative work is supported by: Seton Hall: University Research Council. Ohio University: DOE-BES Grant No. DE-FG02-06ER46317 and NSF Grant No. 0730257. UT Austin: NSF Grant Nos. DMR-0605828 and DGE-0549417, Welch Foundation Grant No. F-1191.

REFERENCES

[1] S. Sonoda, S. Shimizu, T. Sasaki, Y. Yamamoto, H. Hori, J. Crys. Growth **237**, 1358 (2002).

[2] M. L. Reed, N. A. El-Masry, H. H. Stadelmaier, M. K. Ritums, C. A. Parker, J. C. Roberts, S. M. Bedair, Appl. Phys. Lett. **79**, 3473 (2001).

[3] N. Theodoropoulou, K. P. Lee, M. E. Overberg, S. N. G. Chu, A. F. Hebard, C. R. Abernathy, S. J. Pearton, and R. G. Wilson, J. Nanosci. Nanotechnol. **1**, 101 (2001).

[4] G. T. Thaler, M. E. Overberg, B. Gilla, R. Frazier, C. R. Abernathy, S. J. Pearton, J. S. Lee, S. Y. Lee, Y. d. Park, Z. G. Khim, J. Kim, and F. Ren, Appl. Phys. Lett. **80**, 3964 (2002).

[5] M. B. Haider, C. Constantin, H. Al-Brithen, H. Yang, E. Trifan, D. Ingram, A. R. Smith, C. V. Kelly, and Y. Ijiri, J. Appl. Phys. **93**, 5274 (2003).

[6], M. E. Overberg, C. R. Abernathy, S. J. Pearton, N. A. Theodoropoulou, K. T. McCarthy, and A. F. Hebard, Appl. Phys. Lett. **79**, 1312 (2001).

[7] M. B. Haider, C. Constantin, H. Al-Brithen, G. Caruntu, C. J. O'Conner, A. R. Smith, Phys. Stat. Solidi A **202:6**, 1135 (2005).

[8] K. Sato, W. Schweika, P. H. Dederichs, and H. Katayama-Yoshida, Phys. Rev. B **70**, 201202 (2004).

[9] H. Ohno, Science **281**, 951-956 (1998).

[10] K.Y. Wang, R. P. Champion, K. W. Edmonds, M. Sawicki, T. Dietl, C. T. Foxon, B. L. Gallagher, AIP Conf. Proc. **772**, 333-334 (2005).

[11] T. Jungwirth, K. Y. Wang, J. Masek, K. W. Edmonds, J. Konig, J. Sinova, M. Polini, N. A. Goncharuk, A. H. MacDonald, M. Sawicki, A. W. Rushforth, R. P. Campion, L. X. Zhao, C. T. Foxon, B. L. Gallagher, Phys. Rev. B **72 (16)**, 165204-13 (2005).

[12] K. M. Yu, W. Walukiewicz, T. Wojtowicz, W. L. Lim, X. Liu, Y. Sasaki, M. Dobrowolska, J. K. Furdyna, Appl. Phys. Lett. **81**, 844 (2002).

[13] H. A. Al-Brithen, A. R. Smith, D. Gall, Physical Review B **70(4)**, 045303 (2004).

[14] W. R. Lambrecht, Phys. Rev. B **62**, 13538 (2000).

[15] C. Stampfl, W. Mannstadt, R. Asahi, and A. J. Freeman, Phys. Rev. B **63**, 155106 (2001).

[16] H. A. Al-Brithen, E. M. Trifan, D. C. Ingram, A. R. Smith, and D. Gall, J. Cryst. Growth **242**, 345 (2002).

[17] A. R. Smith, H. A. H. Al-Brithen, D. C. Ingram, and D. Gall, J. Appl. Phys. **90**, 1809 (2001).

[18] D. Gall, I. Petrov, L. D. Madsen, J. E. Sundgren, and J. E. Greene, Vac. Sci. Technol. **A 16**, 2411 (1998).

[19] H. A. AL-Brithen, H. Yang, A. R. Smith, J. Appl. Phys. **96(7)**, 3787 (2004).

[20]A. Herwadkar, W. R. L. Lambrecht, Phys. Rev. B **72 (23)**, 235207 (2005).

[21]A. Herwadkar, W. R. L. Lambrecht, M. van Schilfgaarde, Phys. Rev. B **77**, 134433 (2008).

[22] A. Houari, S.F. Matar, M. A. Belkhir, Comp. Mat. Sci. **43 (2)**, 392 (2008).

[23] "Structural, magnetic and electronic properties of dilute MnScN(001) grown by rf nitrogen plasma molecular beam epitaxy" C. Constantin, K. Wang, A. Chinchore, A. R. Smith, H-J. Chia, John Markert, submitted to J. Phys. D: Appl. Phys.